



Molecular Crystals and Liquid Crystals Incorporating Nonlinear Optics

Publication details, including instructions for authors and
subscription information:

<http://www.tandfonline.com/loi/gmcl17>

Nonlinear Optical Properties of Bacteriorhodopsin: Assignment of Second Order Hyperpolarizabilities of Randomly Oriented Systems Using Two-Photon Spectroscopy

R. R. Birge^a, P. A. Fleitz^a, A. F. Lawrence^a, M. A. Masthay^a &
C. F. Zhang^a

^a Department of Chemistry and Center for Molecular Electronics,
Syracuse University Syracuse, New York, 13244
Version of record first published: 22 Sep 2006.

To cite this article: R. R. Birge, P. A. Fleitz, A. F. Lawrence, M. A. Masthay & C. F. Zhang
(1990): Nonlinear Optical Properties of Bacteriorhodopsin: Assignment of Second Order
Hyperpolarizabilities of Randomly Oriented Systems Using Two-Photon Spectroscopy, *Molecular
Crystals and Liquid Crystals Incorporating Nonlinear Optics*, 189:1, 107-122

To link to this article: <http://dx.doi.org/10.1080/00268949008037226>

PLEASE SCROLL DOWN FOR ARTICLE

Full terms and conditions of use: <http://www.tandfonline.com/page/terms-and-conditions>

This article may be used for research, teaching, and private study purposes. Any
substantial or systematic reproduction, redistribution, reselling, loan, sub-licensing,
systematic supply, or distribution in any form to anyone is expressly forbidden.

The publisher does not give any warranty express or implied or make any
representation that the contents will be complete or accurate or up to date. The
accuracy of any instructions, formulae, and drug doses should be independently
verified with primary sources. The publisher shall not be liable for any loss, actions,
claims, proceedings, demand, or costs or damages whatsoever or howsoever caused
arising directly or indirectly in connection with or arising out of the use of this material.

Nonlinear Optical Properties of Bacteriorhodopsin: Assignment of Second Order Hyperpolarizabilities of Randomly Oriented Systems Using Two-Photon Spectroscopy

R. R. BIRGE, P. A. FLEITZ, A. F. LAWRENCE, M. A. MASTHAY and C. F. ZHANG

*Department of Chemistry and
 Center for Molecular Electronics,
 Syracuse University
 Syracuse, New York 13244*

We demonstrate that the second order hyperpolarizability of a randomly oriented molecule can be determined directly from two-photon spectroscopic measurements on the low-lying excited state manifold. Equations are derived which allow not only a determination of β , but also a determination of the error associated with the numerical method. We apply our two-photon technique to an analysis of the second order hyperpolarizability of light adapted bacteriorhodopsin. Our analysis of this protein in D_2O at ambient temperature yields a value of β ($= \beta_{xxx} + (1/3)[\beta_{xyy} + 2\beta_{yyx} + \beta_{xzz} + 2\beta_{zzx}]$) of $(2250 \pm 240) \times 10^{-30} \text{ cm}^5/\text{esu}$ for a laser wavelength of 1.06μ (Nd:YAG fundamental). The large second-order nonlinear properties of bacteriorhodopsin are due primarily to the large change in dipole moment associated with excitation into the lowest-lying strongly allowed ${}^1B_u^{+}$ π, π^* state ($\Delta\mu = 13.5 \pm 0.8 \text{ D}$). We derive an equation which estimates $\Omega_{\beta\beta}$, the ratio of the number of second harmonic photons generated by the system divided by the number of photons absorbed by the system via two-photon processes. Our analysis indicates that molecular doublers can be optimized by maximizing the oscillator strength of the low-lying charge transfer state (f_{so}), the orientation angle of the transition dipole with the polarization of the laser flux, the sample length and the chromophore concentration. All of the above manipulations will also increase the efficiency of doubling, and thus optimization of these parameters is critical to overall doubling performance.

I. INTRODUCTION

Recent studies have demonstrated the significant potential of oriented organic molecules and non-centrosymmetric organic crystals in second harmonic generations.^{1–11} Despite this potential, however, relatively few systematic studies of structure-function relationships have been carried out with the goal of delineating the specific molecular properties that are required in order to optimize the second order hyperpolarizability.^{1–3,8,10–12} This observation is due in part to the difficulty of experimentally measuring the second order hyperpolarizability, β .

Second harmonic generation requires either a non-centrosymmetric crystal or an oriented sample. Most experimental measurements of β use electric field induced second harmonic (EFISH) procedures, and the measured quantity, $I_{2\omega}$, is a complex function of many parameters.^{8,11}

$$I_{2\omega}^{1/2} \propto N f^0(f^\omega)^2 f^{2\omega} \exp[-(\alpha_\omega + \alpha_{2\omega})\ell] \left(\gamma + \frac{\beta\mu}{5kT} \right) \times \{\cosh[(\alpha_\omega - \alpha_{2\omega})\ell] - \cos(\Delta k\ell)\} E_0 I_\omega \quad (1)$$

where N is the number density of the solute, f^* is the local field at frequency κ , α_κ is the absorption coefficient at frequency κ , ℓ is the path length of the cell, γ is the third order hyperpolarizability, β is the second order hyperpolarizability, μ is the ground state static dipole moment, $\Delta k\ell$ is the phase mismatch between the free and the bound waves in the liquid, E_0 is the amplitude of the applied electric field, and I_ω is the intensity of the incident laser irradiation at frequency ω . The relevant components of the second and third order hyperpolarizabilities are given by:

$$\beta = \beta_{xxx} + (1/3)[\beta_{xyy} + 2\beta_{yyx} + \beta_{zzz} + 2\beta_{zzx}] \quad (2)$$

$$\gamma = (1/5)[\gamma_{xxxx} + \gamma_{yyyy} + \gamma_{zzzz} + 2\gamma_{yyzz} + 2\gamma_{zzxx} + 2\gamma_{xxyy}] \quad (3)$$

The above equations assume that the x axis is aligned along the dipole moment vector. Although dilution extrapolation techniques can be used to determine $\beta\mu$ with an accuracy of about $\pm 15\%$ if $\beta\mu \gg \gamma$, decomposition of this product to find β still requires measurement of the static dipole moment.¹¹ Normally the ground state dipole moment is determined by using permittivity measurements, and such techniques are also limited to accuracies of about $\pm 15\%$.¹³ Thus, the typical RMS experimental error in β is $\sim 20\%$. In less favorable circumstances, the error can be many times larger. Although these comments should not be interpreted to suggest that EFISH techniques are not reliable, the techniques that must be adopted in order to minimize error combine to yield a time consuming and error prone experimental procedure. There are also numerous cases when EFISH techniques are incapable of measuring β . Examples particularly relevant to the present study include organic or organometallic salts as well as proteins which carry a net charge. Application of an external field to a solution containing these solutes will typically generate charge migration rather than *in situ* orientation, and under such circumstances, Equation 1 cannot be used to assign β .

The present investigation assigns the second order hyperpolarizability of bacteriorhodopsin by using a technique that does not require the application of an external field. Bacteriorhodopsin has recently received a great deal of attention as a potential component in optically coupled molecular electronic devices.^{6,14–20} The second order hyperpolarizability is an important parameter in defining the potential of this protein to serve in functions that involve second order harmonic generation, electric field induced spatial light modulation, and optical coupling. The measure-

ment of the second order hyperpolarizability, β , is normally accomplished by using electric field induced second harmonic (EFISH) generation. Such experiments are difficult to interpret with respect to a protein bound chromophore. Because most proteins (including bR) carry a net charge, the application of an electric field to a solution containing a protein is likely to induce migration rather than orientation. Even in those cases where the pH of the solution can be adjusted to generate the isoelectric point (no net charge on the protein), the external field causes orientation of the protein determined by the location of the charged amino acids rather than the static dipole moment of the chromophore. Under such circumstances, the use of EFISH to assign β requires assignment of the net orientation and the internal fields, and these assignments are difficult because the normal expansions that are used for small, nearly spherical molecules¹¹ do not apply.

A recent study of bacteriorhodopsin in oriented polyvinyl alcohol (PVA) matrices by Huang *et al.* measured the second order hyperpolarizability to be 2500×10^{-30} cm⁵/esu for 1.06 μ (Nd:YAG fundamental) laser excitation.⁶ A comparison of this value with the β values measured for other molecular systems at the same laser wavelength indicates that if the Huang *et al.* measurement is correct, bacteriorhodopsin has unusual nonlinear properties. These authors noted that a number of tentative assumptions were made in order to convert the measured second harmonic intensity into a value for β , however, one key assumption was the chromophore orientation angle, ζ , that is required in order to convert the measured value of χ^2 into the molecular β ,

$$\chi^2 = N (f^\omega)^2 f^{2\omega} \beta [\cos(\zeta)]^3 \quad (4)$$

Because the mechanism and geometry of *in situ* protein orientation in PVA was unknown, accurate assignment of ζ was not possible. It was assumed that ζ equaled 30°, but this value is likely to have an error range of at least $\pm 15^\circ$. The value of β is very sensitive to the orientation angle (e.g. $\beta[\zeta = 15^\circ] = 1800 \times 10^{-30}$; $\beta[\zeta = 45^\circ] = 4600 \times 10^{-30}$ cm⁵/esu). A second source of error involves uncertainty in the assignment of the internal field functions $[(f^\omega)^2 f^{2\omega}]$. Huang *et al.* assumed Lorentz local field factors and nominal values for the refractive indices of the protein. The inhomogeneity of a protein binding site can produce very large local fields which cannot be predicted accurately by using homogeneous reaction field procedures. We conclude that despite the elegant experimental approach adopted by Huang *et al.*, the lack of detailed orientational and binding site data precludes a definitive assignment of β based on χ^2 measurements. Fortunately, if one can measure experimentally the two-photon absorptivity of the low-lying strongly allowed state, one can assign the second order hyperpolarizability with good precision. We develop the theoretical background for the approach below, and follow the theoretical presentation with an assignment of β for light adapted bacteriorhodopsin. First, however, we will provide a brief overview of the properties of this protein.

Bacteriorhodopsin (MW $\approx 26,000$) is the light transducing protein in the purple membrane of *Halobacterium halobium*.²¹⁻²⁴ The purple membrane, which contains the protein bacteriorhodopsin in a 3:1 protein:lipid matrix, is grown by the bacterium when the concentration of oxygen becomes too low to sustain the generation

of ATP via oxidative phosphorylation. The absorption of light by the light adapted protein initiates a photocycle (Figure 1) which pumps protons from the inside (cytoplasmic) to the outside (extracellular) of the membrane. The resulting pH gradient ($\Delta\text{pH} \sim 0.2$) generates a proton-motive force which is used to synthesize ATP from inorganic phosphate and ADP. *Halobacterium halobium* is thus capable of either respiratory or photochemical ATP synthesis. Bacteriorhodopsin has been the subject of numerous spectroscopic investigations during the past decade, not only because of its unique biochemistry,^{21,24,25,26} but also because of its unique photophysical properties.²⁷ The two-photon double-resonance spectrum of light adapted bacteriorhodopsin in D₂O at room temperature is shown in Figure 2.²⁸ This spectrum is unique relative to other two-photon spectra measured for the visual chromophores and pigments^{29–35} in that it exhibits two low-lying band maxima. The lowest energy band maximum at 560nm ($\delta = 290 \text{ GM}$) corresponds within experimental error with the one-photon absorption maximum at 568nm, and is assigned to the $^1\text{B}_u^+ \leftarrow \text{S}_0$ transition. The higher energy two-photon band at $\sim 488\text{nm}$ ($\delta = 120 \text{ GM}$) does not correspond to a resolved one-photon feature and

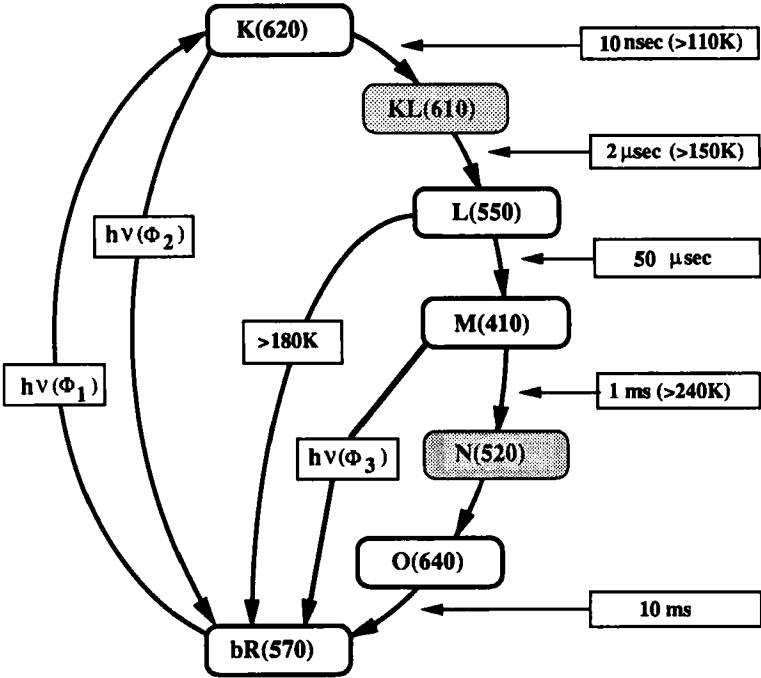


FIGURE 1 Photocycle of light-adapted bacteriorhodopsin. Individual species are indicated within the polygons and the numbers in parentheses following the labels indicate the approximate absorption maximum in nanometers extrapolated to ambient temperature aqueous environment. Species within shaded polygons are tentative and/or are not observed under all experimental conditions. Relative free energies are related approximately to vertical position. Temperatures required for observing the formation of subsequent intermediates and formation times extrapolated to ambient temperature are indicated for selected reactions, and are very approximate. A few key thermal and photochemical branching reactions are shown.

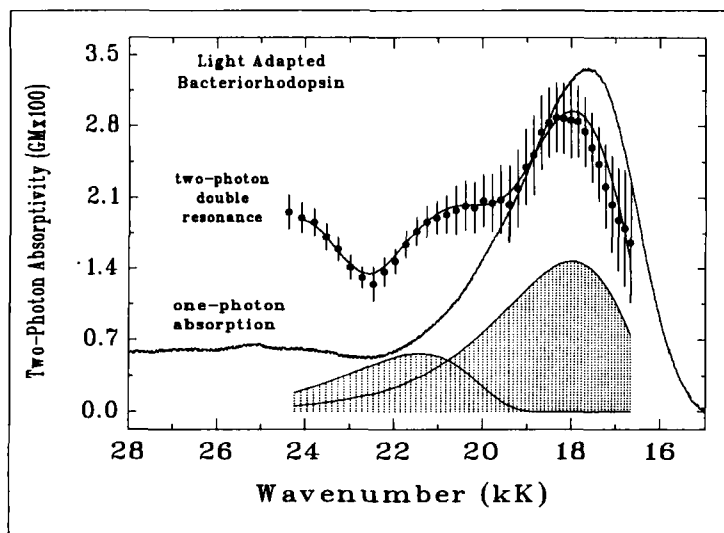


FIGURE 2 Comparison of the two-photon double resonance spectrum with the one-photon absorption spectrum of light-adapted bacteriorhodopsin in D_2O at ambient temperature. The height of the vertical error bar on each of the two-photon data points is equal to the standard deviation of the two-photon signal determined via least-squares regression of the double-resonance signal as a function of laser pulse energy. The solid line through the two-photon data was fit to the data by using log-normal regression assuming $\rho = 1.60$ and restricting all full-widths at half maxima to identical values. The fit predicts the following results: lowest energy band (${}^1B_u^{*+} \leftarrow \leftarrow S_0$ transition) [$\tilde{\nu}_{\max} = 17975 \text{ cm}^{-1}$; $\tilde{\nu}_{\text{fwhm}} = 3420 \text{ cm}^{-1}$; $I_{\text{rel}} = 0.9997$]; band 2 (${}^1A_g^{*-} \leftarrow \leftarrow S_0$ transition) [$\tilde{\nu}_{\max} = 21406 \text{ cm}^{-1}$; $\tilde{\nu}_{\text{fwhm}} = 3420 \text{ cm}^{-1}$; $I_{\text{rel}} = 0.404$]; band 3 (see below [$\tilde{\nu}_{\max} = 24584 \text{ cm}^{-1}$; $\tilde{\nu}_{\text{fwhm}} = 3420 \text{ cm}^{-1} = 0.597$]). The resulting log-normal distributions for bands 1 and 2 are displayed at half maximum intensity in the filled in spectra at the bottom of the figure. The third band was included in the fit to remove contributions from higher energy two-photon transitions that contribute to the higher energy regions of the spectrum, and as such, is not considered to have physical significance.

is assigned to the ${}^1A_g^{*-} \leftarrow S_0$ transition. Not only is it surprising to find that both the ${}^1A_g^{*-}$ and ${}^1B_u^{*+}$ states generate discernable two-photon maxima, but the observation that the ${}^1B_u^{*+}$ state two-photon absorptivity is more than twice as large as that associated with the ${}^1A_g^{*-}$ deserves special notice. This result indicates that the two-photon absorptivities are dominated by initial and final state contributions (see discussion in Reference 34), and thus the two-photon absorptivity is proportional to the change in dipole moment upon excitation into the final state. A detailed analysis yields $\Delta\mu$ (${}^1B_u^{*+}$) = $13.5 \pm 0.8 \text{ D}$ and $\Delta\mu$ (${}^1A_g^{*-}$) = $9.1 \pm 4.8 \text{ D}$.²⁸ Thus, the low-lying, strongly allowed ${}^1B_u^{*+}$ state is a $\pi^* \leftarrow \pi$ charge transfer state that has long been recognized as a key contributor to the second order molecular hyperpolarizability of conjugated molecules.¹⁻¹¹

The intrinsic properties of the native protein make it an outstanding candidate for use in optical switching, optical RAM and optical associative memory applications.^{14-17,20,36-41} These properties include (1) long term stability of the protein to thermal and photochemical degradation, (2) picosecond photochemical reaction times (both the forward and reverse photoreactions produce stable products in less

than 5 picoseconds at 77K), (3) high forward and reverse quantum yields permitting the use of low light levels for switching, (4) wavelength independent quantum yields, (5) a large shift in absorption spectrum accompanying photochemistry which permits accurate and reproducible assignment of state, (6) high two-photon cross sections for photoactivation permitting higher storage densities than is possible via one-photon excitation and (7) the ability to form thin films of bacteriorhodopsin with excellent optical properties by using Langmuir-Blodgett or spin-coating techniques. We demonstrate in this paper that bacteriorhodopsin also has some unique nonlinear optical properties.

II. RESULTS AND DISCUSSION

The key theoretical goal of this paper is to demonstrate that under near resonance conditions, the measurement of the two-photon absorptivity can provide a direct experimental determination of the second order hyperpolarizability. To understand the origin of this relationship, it is useful to compare the expansion which describes the molecular polarization, P_i , with the expansion which describes the probability of photon absorption, P_ω :

$$P_i = \alpha_{ij} \cdot E_j + \beta_{ijk} \cdot E_j E_k + \dots \quad (5)$$

$$P_\omega = \sigma_\omega(NL) + \delta_\omega(FSNL) + \dots \quad (6)$$

where α_{ij} is the molecular polarizability, E_i is the applied electric field in the i direction, σ_ω is the one-photon cross section, δ_ω is the two-photon absorptivity, N is the number density of the absorber, L is the path length, F is the photon flux and S is two-photon coherence function.⁴² Although the molecular parameters that appear in these two expansions may appear to have little if any relationship, closer inspection indicates that under "near-resonance" conditions, the terms start to converge with respect to dependence on key molecular one- and two-electron integrals. Let us examine this issue from the perspective of the leading terms α_{ij} and σ_ω . The one-photon cross-section is proportional to the following sum:

$$\sigma_\omega \propto \sum_{k=1}^N g_k^{(1)}(\omega) \omega |\langle k | \mathbf{e} \cdot \mathbf{r} | 0 \rangle|^2 \quad (7)$$

where $g_k^{(1)}(\omega)$ is the one-photon vibronic line-shape function for the k th excited state, ω is the frequency of the irradiation, $\langle k | \mathbf{e} \cdot \mathbf{r} | 0 \rangle$ is the transition moment associated with $k \leftarrow 0$ transition, and the summation is over all N excited states. In practice, only a few excited states contribute to the absorption process, and the selection of which excited states contribute is a function of the line-shape functions, which represent the unitless, normalized vibronic distributions of the excited states. The molecular electronic polarizability is defined by:

$$\alpha_{ij} \propto \sum_{k=1}^N \left(\frac{\langle o|e|i\rangle\langle k|e|j\rangle}{\omega_{ko} - \omega} + \frac{\langle o|e|j\rangle\langle k|e|i\rangle}{\omega_{ko} + \omega} \right) \quad (8)$$

It is clear by inspection that both α and σ depend upon the same molecular integrals and stationary state energies, but the knowledge of one will not necessarily permit determination of the other because of the different energetic weighting factors. Only when $\omega_{io} - \omega$ approaches zero (so that $\langle o|e|i\rangle\langle i|e|\psi\rangle$ dominates the sum in Equation 8) and $g_i^{(1)}(\omega)$ dominates (so that $\langle k|e|r\rangle$ dominates the sum in Equation 7) can α and σ be functionally related to one another. We do not explore this issue in further detail here, because a full derivation is peripheral to our principal goal. Nevertheless, the above example illustrates the effect that a near-resonance will have on the relationship between α and σ . A similar, though much more complicated relationship can be established linking β and δ . This is the goal of the remainder of this section.

II-A. Perturbation treatment of the two-photon absorption process

The two-photon absorptivity of the s th excited state is a function not only of the properties of the molecule but also the laser polarization and energies used to generate a simultaneous two-photon absorption in the molecule.⁴²

$$\delta_v^{so} = \frac{8\pi^4 e^4}{(ch)^2} \bar{\nu}_\lambda \bar{\nu}_\mu g(\bar{\nu}_\lambda + \bar{\nu}_\mu) |S_{so}(\lambda, \mu)|^2 \quad (9)$$

where $\bar{\nu}_\lambda$ and $\bar{\nu}_\mu$ are the frequencies of the two laser beams, $g(\bar{\nu}_\lambda + \bar{\nu}_\mu)$ is the normalized lineshape function (see below) and $S_{so}(\lambda, \mu)$ is the two-photon tensor:

$$S_{so}(\alpha, \beta) = \sum_{j=0}^N \left(\frac{\alpha \cdot \langle i|r|o \rangle \langle s|r|i \rangle \cdot \beta}{\bar{\nu}_j - \bar{\nu}_\alpha + i\Gamma_j} + \frac{\beta \cdot \langle i|r|o \rangle \langle s|r|i \rangle \cdot \alpha}{\bar{\nu}_j - \bar{\nu}_\beta + i\Gamma_j} \right) \quad (10)$$

where α and β are the unit vectors defining the polarization of the two photons and $\bar{\nu}_j$ and Γ_j are the transition frequency and the homogeneous linewidth of state j , respectively. As we examine in more detail below, the summation is over all electronic states of the molecule including the ground and final states.⁴³ Equation 9 includes a factor of 1/2 that is required in order to make the theoretical and the experimental definitions identical.⁴⁴ The normalized lineshape function will be approximated for the present analysis by using a log-normal distribution:^{30,45,46}

$$g(\bar{\nu}_\mu + \bar{\nu}_\lambda) = g_{\max} \exp - \left\{ \frac{\ln 2}{(\ln \rho)^2} \left[\ln \left(\frac{\bar{\nu}_\mu + \bar{\nu}_\lambda - \bar{\nu}_{so}(\rho^2 - 1)}{\Delta \bar{\nu} \rho} + 1 \right) \right]^2 \right\} \quad (11a)$$

$$\bar{\nu}_\mu + \bar{\nu}_\lambda > \bar{\nu}_{so} - [\Delta \bar{\nu} \rho / (\rho^2 - 1)], \quad (11a)$$

$$g(\bar{\nu}_\mu + \bar{\nu}_\lambda) = 0, \quad \bar{\nu}_\mu + \bar{\nu}_\lambda \leq \bar{\nu}_{so} - [\Delta \bar{\nu} \rho / (\rho^2 - 1)] \quad (11b)$$

where,

$$g_{\max} = \left(\frac{4 \ln 2}{\pi c^2 \Delta \tilde{\nu}^2} \right)^{1/2} \left\{ \frac{2 \rho(\ln \rho)}{(\rho^2 - 1)} \exp \left(\frac{(\ln \rho)^2}{4 \ln 2} \right) \right\}^{-1}, \quad (12)$$

$\tilde{\nu}_{\text{so}}$ is the wavenumber at maximum two-photon absorptivity, $\Delta \tilde{\nu}$ is the full-width at half-maximum (FWHM) in wavenumbers and ρ is the skewness. The units of g (sec) derive from the fact that this function is normalized to unity in frequency space.⁴⁶ The skewness is a dimensionless parameter which is an indirect measure of the distribution of vibronic activity into higher vibrational modes due to Franck-Condon activity, vibronic coupling and/or vibronic resonance effects. A log-normal fit to the two-photon double resonance spectrum is shown in Figure 2, and yields a value of g_{\max} for all bands of 8.828×10^{-15} sec ($\rho = 1.6$, $\Delta \tilde{\nu} = 3420 \text{ cm}^{-1}$).

The two-photon absorptivity of one-photon allowed excited states in polar molecules is invariably dominated by the initial and final state contributions to the summation over intermediate states in Equation 10.^{32,–34,42,47–50} Under these circumstances, the two-photon allowedness is determined primarily by the change in dipole moment between the ground and final states. The following equation includes this contribution, as well as the i th intermediate state contribution, to the total two-photon absorptivity:

$$\delta_{\max}^{s \leftarrow 0} = \frac{4\pi^4 e^4 \tilde{\nu}_\lambda^2}{15c^2 h^2} g_{\max} \left\{ \frac{(a + b) [\langle i|\mathbf{r}|\mathbf{o}\rangle \cdot \langle s|\mathbf{r}|i\rangle]^2}{(\tilde{\nu}_{\text{io}} - \tilde{\nu}_\lambda)^2} + \frac{b |\langle i|\mathbf{r}|\mathbf{o}\rangle|^2 |\langle s|\mathbf{r}|i\rangle|^2}{(\tilde{\nu}_{\text{io}} - \tilde{\nu}_\lambda)^2} \right\} \quad (13a)$$

$$+ \frac{8\pi^4 e^3 \tilde{\nu}_\lambda^2}{15c^2 h^2} g_{\max} \left\{ \frac{(a + 2b) \langle i|\mathbf{r}|\mathbf{o}\rangle \langle s|\mathbf{r}|i\rangle \langle s|\mathbf{r}|\mathbf{o}\rangle \|\Delta\mu_{\text{so}}\| \cos(\phi_{\text{ave}})^2}{(\tilde{\nu}_{\text{io}} - \tilde{\nu}_\lambda)} \right\} \quad (13b)$$

$$+ \frac{4\pi^4 e^2}{15c^2 h^2} g_{\max} \{ (a + b) (\Delta\mu_{\text{so}} \cdot \langle s|\mathbf{r}|\mathbf{o}\rangle)^2 + b \Delta\mu_{\text{so}}^2 |\langle s|\mathbf{r}|\mathbf{o}\rangle|^2 \}, \quad (13c)$$

where

$$\Delta\mu_{\text{so}} = \mu_s - \mu_o. \quad (14)$$

and a and b are photon polarization and propagation variables (see References 46 and 51) and ϕ_{ave} is the RMS average of the following ten transition/dipole vector angles with the specified weightings: $\langle i|\mathbf{r}|\mathbf{o}\rangle \langle s|\mathbf{r}|i\rangle$, $\langle s|\mathbf{r}|\mathbf{o}\rangle \Delta\mu_{\text{so}}$, $2\langle i|\mathbf{r}|\mathbf{o}\rangle \Delta\mu_{\text{so}}$, $2\langle s|\mathbf{r}|\mathbf{o}\rangle \langle s|\mathbf{r}|i\rangle$, $2\langle s|\mathbf{r}|\mathbf{o}\rangle \langle i|\mathbf{r}|\mathbf{o}\rangle$, $2\langle s|\mathbf{r}|i\rangle \Delta\mu_{\text{so}}$. The cross term in Equation 13b has been simplified and is rigorous only when $\phi_{\text{ave}} = 0$. We can informally describe Equation 13 as dividing the two-photon absorption process into three contributions, an electronic term (13a), a dipolar (or charge transfer) term (13c) and a cross term (13b).

II-B. Perturbation treatment of the second order hyperpolarizability

The second order hyperpolarizability is given by the following expansion:^{1,8,9,11,52,53}

$$\beta_{ijk}^{2\omega} + \beta_{ikj}^{2\omega} = \frac{-e^3}{4} \sum_r \sum_s \left\{ \frac{\langle o|j|s\rangle \langle s|i|r\rangle \langle r|k|o\rangle + \langle o|k|s\rangle \langle s|i|r\rangle \langle r|j|o\rangle}{(\Delta E_{so} - E_\lambda + i\Gamma_s)(\Delta E_{ro} + E_\lambda + i\Gamma_r)} \right. \\ + \frac{\langle o|j|s\rangle \langle s|i|r\rangle \langle r|k|o\rangle + \langle o|k|s\rangle \langle s|i|r\rangle \langle r|j|o\rangle}{(\Delta E_{so} + E_\lambda + i\Gamma_s)(\Delta E_{ro} - E_\lambda + i\Gamma_r)} \\ + \frac{\langle o|i|s\rangle \langle s|j|r\rangle \langle r|k|o\rangle + \langle o|i|s\rangle \langle s|k|r\rangle \langle r|j|o\rangle}{(\Delta E_{so} + 2E_\lambda + i\Gamma_s)(\Delta E_{ro} + E_\lambda + i\Gamma_r)} \\ + \frac{\langle o|i|s\rangle \langle s|j|r\rangle \langle r|k|o\rangle + \langle o|i|s\rangle \langle s|k|r\rangle \langle r|j|o\rangle}{(\Delta E_{so} - 2E_\lambda + i\Gamma_s)(\Delta E_{ro} - E_\lambda + i\Gamma_r)} \\ + \frac{\langle o|j|s\rangle \langle s|k|r\rangle \langle r|i|o\rangle + \langle o|k|s\rangle \langle s|j|r\rangle \langle r|i|o\rangle}{(\Delta E_{so} - E_\lambda + i\Gamma_s)(\Delta E_{ro} - 2E_\lambda + i\Gamma_r)} \\ \left. + \frac{\langle o|j|s\rangle \langle s|k|r\rangle \langle r|i|o\rangle + \langle o|k|s\rangle \langle s|j|r\rangle \langle r|i|o\rangle}{(\Delta E_{so} + E_\lambda + i\Gamma_s)(\Delta E_{ro} + 2E_\lambda + i\Gamma_r)} \right\} \quad (15)$$

where the off-diagonal elements, $\langle s|ej|r\rangle$ ($s \neq r$), are the transition moments coupling the s th and r th states, and the diagonal element, $\langle r|ej|r\rangle$, represents the dipole moment of the r th state relative to the ground state. Thus, $\langle o|ej|o\rangle$ is defined to be zero, which requires a charge centroid based analysis.⁵³ In practice, the ground state dipole moment components are simply subtracted from all the corresponding components of the diagonal integrals prior to evaluating the expansion. Equation 15 includes a damping constant, Γ_ρ , which is important to include when the energy of the laser photons, E_λ , approaches one-half of the transition energy of an allowed excited state. These damping constants are formally equal to the homogeneous linewidth, but larger values are often adopted in order to simulate the effect of inhomogeneous broadening. We will explore these damping options in further detail below.

Under conditions where the two-photon absorptivity of the low-lying strongly allowed excited state is dominated by initial and final state contributions, the second order hyperpolarizability, β , is related to the two-photon absorptivity by the following relationship:

$$\beta = \beta_{xxx} + (1/3)[\beta_{xyy} + 2\beta_{yyx} + \beta_{xzz} + 2\beta_{zzx}] \quad (16a)$$

$$= \xi_{\beta 1} - \xi_{\beta 2} + \xi_{\beta 3} \quad (16b)$$

$$\xi_{\beta 1} = \frac{15^{1/2} c e h^2}{32 \pi^3 m_e^{1/2}} \left\{ \frac{(\delta_{\max}^{s \leftarrow o})^{1/2} f_{so}^{1/2} E(\Delta E_{so}, \Gamma_s, E_\lambda)}{g_{\max}^{1/2}} \right\} \quad (16c)$$

$$\xi_{\beta 2} = \frac{3 e^3 h^2}{16 \pi^2 m_e} \left\{ \frac{\Delta E_{so}^{1/2} f_{so}^{1/2} \langle s|r|i \rangle E(\Delta E_{so}, \Gamma_s, E_\lambda)}{E_\lambda [2\Delta E_{io} - \Delta E_{so}]} \right\} \quad (16d)$$

$$\xi_{\beta 3} = \frac{3 e^3 h^2}{8 \pi^2 m_e} \left\{ \frac{\Delta E_{ave}^{1/2} f_{so}^{1/2} f_{io}^{1/2} \langle s|r|i \rangle E(\Delta E_{ave}, \Gamma_{ave}, E_\lambda)}{E_\lambda \Delta E_{io}^{1/2} \Delta E_{so}^{1/2}} \right\} \quad (16e)$$

where

$$E(\Delta E_{\rho\sigma}, \Gamma_\rho, E_\lambda) =$$

$$\left\{ \frac{9E_\lambda^2 \Delta E_{\rho\sigma}^3 + 4E_\lambda^4 \Gamma_\rho + 14E_\lambda^2 \Delta E_{\rho\sigma} \Gamma_\rho^2 + \Delta E_{\rho\sigma}^3 \Gamma_\rho^2 + 5E_\lambda^2 \Delta E_{\rho\sigma} \Gamma_\rho^3 + 2\Delta E_{\rho\sigma} \Gamma_\rho^4 + \Gamma_\rho^5}{(\Gamma_\rho^2 + (\Delta E_{\rho\sigma} - 2E_\lambda)^2) (\Gamma_\rho^2 + (\Delta E_{\rho\sigma} - E_\lambda)^2) (\Gamma_\rho^2 + (\Delta E_{\rho\sigma} + E_\lambda)^2) (\Gamma_\rho^2 + (\Delta E_{\rho\sigma} + 2E_\lambda)^2)} \right\}^{1/2} \quad (17)$$

$\Delta E_{ave} = \frac{1}{2} (\Delta E_{so} + \Delta E_{io})$, and the $s \leftarrow o$ transition is assigned to the low-lying strongly allowed (charge-transfer) state and the $i \leftarrow o$ transition is assigned to a second low-lying transition which is allowed and couples electronically via $\langle s|r|i \rangle$. For polar polyenes in general, and bacteriorhodopsin in particular, the following assignments apply: $s \equiv {}^1B_u^{*+}$ and $i \equiv {}^1A_g^{*-}$. The term, $E(\Delta E_{\rho\sigma}, \Gamma_\rho, E_\lambda)$, is a function of three energies: $\Delta E_{\rho\sigma}$, the transition energy of the $\rho \leftarrow \sigma$ transition; Γ_ρ , the homogeneous linewidth of the ρ th excited state; and E_λ , the energy of the laser photons.

The $\xi_{\beta 1}$ terms can be used to determine approximately the error that is introduced by truncation of the perturbation expansion to a three level approximation:

$$\beta_{\text{error}}^{\text{truncation}} \approx \frac{\xi_{\beta 1} \xi_{\beta 2}}{2^{1/2} \xi_{\beta 3}} \quad (18)$$

Values of β for light adapted bacteriorhodopsin are presented in Table I for selected values of the damping constant and for two experimentally relevant laser energies [$E_\lambda = 1.17$ eV ($\lambda = 1.06$ μ , the Nd:YAG fundamental), $E_\lambda = 0.654$ eV ($\lambda = 1.9$ μ , the Nd:YAG fundamental Raman shifted by hydrogen gas via the first anti-Stokes line)]. The dispersion of β for E_λ from 0.4 – 1.5 eV is shown in Figure 3. For simplicity, all of our calculations assume that $\Gamma_s = \Gamma_i$, and for reference, we have calculated β for three values that serve to bracket the physically realistic possibilities in Table I. Naturally, the lowest possible value of Γ is zero, which is a reasonable value to use only in non-resonant cases (i.e. $E_\lambda = 0.654$ eV, Table I). An approximate upper limit is $\Gamma = 1000$ cm^{-1} , which is a rough estimate for the inhomogeneous linewidth.^{54,55} The most appropriate value from a formalistic

TABLE I

Second Order Hyperpolarizability (β) and Ratio of Second Harmonic to Two-Photon Absorption Events ($\Omega\beta\delta$) for Light-Adapted Bacteriorhodopsin (D_2O ; 297K)

$E_\lambda(\gamma)^{(a)}$	$\Gamma \text{ (cm}^{-1}\text{)}^{(b)}$	$\beta \text{ (} \times 10^{30} \text{ cm}^5/\text{esu)}^{(c)}$	$\Omega\beta\delta^{(d)}$
1.17 eV (1.06 μ)	0	2430 \pm 210	69,000
1.17 eV (1.06 μ)	250	2250 \pm 240	69,000
1.17 eV (1.06 μ)	1000	1520 \pm 250	69,000
0.654 eV (1.9 μ)	0	330 \pm 130	10,900
0.654 eV (1.9 μ)	250	329 \pm 130	10,900
0.654 eV (1.9 μ)	1000	327 \pm 130	10,900
0.1 eV	250	198	86
0.2 eV	250	203	355
0.3 eV	250	214	993
0.4 eV	250	232	2230
0.5 eV	250	258	4400
0.6 eV	250	299	8040
0.8 eV	250	477	23,500
1.0 eV	250	1480	42,200
1.2 eV	250	2610	83,300
1.4 eV	250	549	133,000
1.6 eV	250	377	176,000
1.8 eV	250	356	253,000

(a) Energy (eV) and wavelength of the laser irradiation for two experimentally common values (1.06 μ = Nd:YAG fundamental; 1.9 μ = first anti-Stokes H_2 Raman shifted line) as well as a series of energies from 0.1–1.8 eV. Underlined values are indicated graphically in Figure 3.

(b) Damping constant (Γ) used in Equations 16 and 17 to calculated β (see text).

(c) Value of β determined by using Equations 16 and 17 and spectroscopic data from Reference 28.

(d) The number of second harmonic photons generated by the oriented sample divided by the number of photons absorbed by the sample via two-photon absorption based on Equations 19 and 20. Parameter assignments are as follows: $L = 1 \text{ cm}$, $\zeta = 0$, $N = 6 \times 10^{20} \text{ cm}^{-3}$, $E_{\text{rwhm}} = 3000 \text{ cm}^{-1}$, $\Delta E_{\text{so}} = 17500 \text{ cm}^{-1}$, $f_{\text{so}} = 0.8$, $n_\lambda = 1.3$, $n_{\lambda/2} = 1.4$.

standpoint is $\Gamma = 250 \text{ cm}^{-1}$, an upper limit to the homogeneous linewidth in bR.⁵⁴ Our two-photon double resonance determination of β for $E_\lambda = 1.17 \text{ eV}$ and $\Gamma = 250 \text{ cm}^{-1}$ yields $\beta = (2250 \pm 240) \times 10^{30} \text{ cm}^5/\text{esu}$, a value in good agreement with the oriented thin film measurement of Huang *et al.*⁶ which gave $\beta = 2500 \times 10^{30} \text{ cm}^5/\text{esu}$. No error range was provided for the latter measurement, but given the uncertainty in the orientation factor (see above), it is surprising that the two values are in such good agreement. The error in our measurement is determined in part by truncation error inherent in Equation 16 [$\xi_{\beta 1} = 1504$, $\xi_{\beta 2} = 118$, $\xi_{\beta 1} = 865$, $\xi_{\beta 1} \xi_{\beta 2} / (2^{1/2} \xi_{\beta 3}) = 145$; all values $\times 10^{30} \text{ cm}^5/\text{esu}$].

II-C. Optimization of molecules for second harmonic generation

The above theoretical treatment indicates that molecules with large second order hyperpolarizabilities will also have the potential for efficient two-photon absorption. Two-photon absorption is a competitive and undersirable process for a doubler, and thus one should design a molecular system to optimize the ratio of doubling to two-photon absorption.

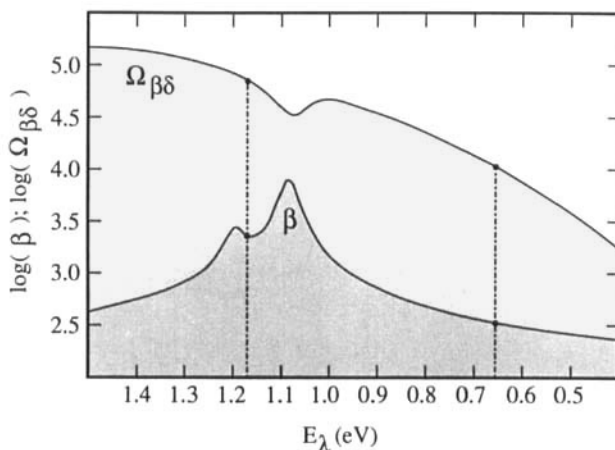


FIGURE 3 Energy dependence of the second order hyperpolarizability (β) and ratio of second harmonic to two-photon absorption events ($\Omega_{\beta\delta}$) for light-adapted bacteriorhodopsin (D_2O ; 297K). Parameter assignments relevant to the calculation of $\Omega_{\beta\delta}$ (Equations 19 and 20) are as follows: L (path length) = 1 cm, ζ (chromophore orientation angle) = 0° , N (protein number density) = $6 \times 10^{20} \text{ cm}^{-3}$, $\Delta E_{\text{fwhm}} = 3000 \text{ cm}^{-1}$, ΔE_{so} (${}^1B_u^+ \leftarrow S_0$ one-photon transition energy) = 17500 cm^{-1} , f_{so} (one-photon oscillator strength) = 0.8, $n_\lambda = 1.3$, $n_{\lambda/2} = 1.4$.

The following relationship, based on the simultaneous solution of Equation 16 (above), Equation 49 (p. 136) from Reference 42 and Equation 16.7-4 (p. 431) from Reference 56 yields an estimate of the dimensionless ratio, $\Omega_{\beta\delta}$, which is defined as the number of second harmonic photons generated by the oriented sample divided by the number of photons absorbed by the sample via two-photon processes:

$$\Omega_{\beta\delta} \equiv \frac{50^{1/2} e^2 h}{432 \ln(2)^{1/2} \pi^{1/2} c m_e} \left\{ \frac{N L f_{\text{so}} \cos(\zeta)^6 (n_\lambda^2 + 2)^4 (n_{\lambda/2}^2 + 2)^2 E_\lambda^3 \Delta E_{\text{so}}^3 (\Delta E_{\text{fwhm}}^2 + 12(2E_\lambda - \Delta E_{\text{so}})^2)^{1/2}}{n_\lambda^3 (4 E_\lambda^4 - 5 E_\lambda^2 \Delta E_{\text{so}}^2 + \Delta E_{\text{so}}^4)^2} \right\} \quad (19)$$

where N is the number density of the chromophore, L is the path length, ζ is the orientation angle defined in Equation 4, E_λ is the energy of the laser photons, n_λ is the refractive index of the solution at the laser wavelength, $n_{\lambda/2}$ is the refractive index of the solution at the second harmonic wavelength, and ΔE_{so} , ΔE_{fwhm} and f_{so} are the transition energy, full-width at half-maximum and oscillator strength of the low-lying charge transfer state. The above equation was derived by making a number of assumptions and approximations which include those adopted in generating Equations 13 and 16 as well as: confocal Gaussian focussing; linearly polarized and off-resonance laser excitation ($\Gamma = 0$ in Equation 17); Lorentzian lineshapes and local fields; and $\xi_{\beta 2} = \xi_{\beta 3}$ (Equation 16). These approximations

probably relegate Equation 19 to “order-of-magnitude” estimates. Nevertheless, Equation 19 provides important insights into what parameters and conditions are important to optimize in order to maximize second harmonic generation relative to two-photon absorption. For example, a key variable is the orientation angle, ζ , the cosine of which appears to the sixth power in Equation 19. Thus, a sample that is perfectly oriented ($\zeta = 0$) will have a performance advantage of ~ 1.5 times that of a sample that has an average misalignment of 20° . This example emphasizes the importance of molecular orientation, and suggests that poling, rather than electric field orientation, will find increased use in the preparation of molecular based doublers. Sample length (L), solute concentration (N) and oscillator strength (f_{so}) all appear to the first order in Equation 19, and to the extent possible, should be optimized to improve performance. The chemist normally has limited flexibility in manipulating sample length (which is typically limited by optical and system considerations). Thus, f_{so} and N become the key variables to manipulate, although the flexibility available in the manipulation of f_{so} is small. Virtually all candidate π -electron systems have large oscillator strengths for the charge transfer state, because this parameter is also important to the generation of large second order hyperpolarizabilities. More interestingly, Equation 19 suggests that concentration has an important role to play, and should be increased to the extent possible to minimize two-photon absorption interference. This observation is contrary to intuition, and supports the use of molecular crystals, rather than polymer bound chromophores, in molecular doubler applications. Finally, it is clear that excited state energy levels play a critical role in determining $\Omega_{\beta\beta}$. Synthetically tuning the transition energy of the low-lying charge transfer state to minimize the expression $(4E_\lambda^4 - 5E_\lambda^2 E_{so}^2 + E_{so}^4)$ will optimize both β and $\Omega_{\beta\beta}$, and if one is designing a molecular doubler for use at only one laser wavelength, this term represents the key expression to minimize. It should be recognized, however, that damping will decrease the effect of this term, and near resonance, Equation 19 should be multiplied by the following dimensionless correction term to reflect accurately the influence of a near resonance on $\Omega_{\beta\beta}$,

$$E_{\#} = (4 E_\lambda^4 - 5 E_\lambda^2 E_{so}^2 + E_{so}^4)^2 (E(\Delta E_{so}, \Delta E_{fwhm}, E_\lambda))^2 / (9 E_\lambda^2 E_{so}^3) \quad (20)$$

where $E(\Delta E_{so}, \Delta E_{fwhm}, E_\lambda)$ is defined in Equation 17. (To properly reflect the use of Lorentzian line shapes, the Γ term in Equation 17 is replaced with ΔE_{fwhm} in the evaluation of $\Omega_{\beta\beta}$.) A dispersion curve of $\Omega_{\beta\beta}$ for light adapted bacteriorhodopsin is shown in Figure 3 based on the use of Equations 19 and 20.

III. SUMMARY AND CONCLUSIONS

(1) We demonstrate that the second order hyperpolarizability of a randomly oriented molecule can be determined directly from two-photon spectroscopic measurements on the low-lying excited state manifold. Equations are derived which allow not only a determination of β , but also the determination of the error as-

sociated with the numerical method. The use of two-photon spectroscopy to determine β is a particularly valuable experimental technique for the analyses of proteins and salts. These molecules tend to migrate rather than orient when external fields are applied, and thus cannot be studied under normal circumstances by using electric field induced second harmonic generation.

(2) We apply our two-photon technique to an analysis of the second order hyperpolarizability of light adapted bacteriorhodopsin. Our analysis of this protein in D_2O at ambient temperature yields a value of β ($= B_{xxx} + (1/3)[\beta_{xyy} + 2B_{yyx} + \beta_{zzz} + 2\beta_{zzx}]$) of $(2250 \pm 240) \times 10^{-30} \text{ cm}^5/\text{esu}$ for a laser wavelength of 1.06μ (Nd:YAG fundamental). The value is enhanced by resonance and a value off-resonance is much lower ($\beta[1.9\mu] = (329 \pm 130) \times 10^{-30} \text{ cm}^5/\text{esu}$). Both values are indicative of a strongly nonlinear material, however, and we assign this characteristic of bacteriorhodopsin to the large change in dipole moment associated with excitation into the lowest-lying strongly allowed ${}^1B_u^{+} \pi, \pi^*$ state ($\Delta\mu = 13.5 \pm 0.8 \text{ D}$).

(3) An equation is derived which estimates the dimensionless ratio, $\Omega_{\beta\delta}$, which is defined as the number of second harmonic photons generated by the oriented sample divided by the number of photons absorbed by the sample via two-photon processes. This term should be optimized in order to minimize competitive two-photon absorption processes. In addition to maximizing resonances, which will not only increase β but also $\Omega_{\beta\delta}$, our analysis indicates that molecular doublers can be optimized by maximizing, via synthesis and/or environmental manipulation, the oscillator strength of the low-lying charge transfer state (f_{so}), and the orientation angle of the transition dipole with the polarization of the laser flux. In addition, the sample length and the solute concentration should be increased to the extent possible. The key variable is the orientation angle, ζ , the cosine of which appears to the sixth power in the expression for $\Omega_{\beta\delta}$. Thus, a sample that is perfectly oriented ($\zeta = 0$) will have a performance advantage of ~ 1.5 times that of a sample that has an average misalignment of 20° . Interestingly, increasing the change in dipole moment upon excitation into the low-lying charge transfer state does not increase $\Omega_{\beta\delta}$. All of the molecular manipulations predicted to increase $\Omega_{\beta\delta}$ will also increase the efficiency of doubling, and thus their manipulation is critical to overall doubling performance.

Acknowledgments

This work was supported in part by grants from the National Institutes of Health (GM-34548), the National Science Foundation (CHE-8516155; STC-8810879) and the Office of Naval Research (N00014-88-K-0359). The authors thank Drs. D. Bloor, D. F. Bocian, A. F. Garito, S. R. Marder, H. Sasabe, and K. D. Singer for interesting and helpful discussions.

References

1. D. S. Chemla and J. Zyss. *Nonlinear optical properties of organic molecules and crystals* (Academic Press, Orlando, Florida, 1987).
2. C. W. Dirk, R. J. Twieg and G. Wagniere, *J. Am. Chem. Soc.* **108**, 5387–5395 (1986).

3. R. A. Hann and D. Bloor, *Organic materials for non-linear optics* (Royal Society of Chemistry, London, England, 1988).
4. J. Y. Huang, A. Lewis and T. Rasing, *J. Phys. Chem.*, **92**, 1756–1759 (1988).
5. J. Y. Huang, A. Lewis and L. Loew, *Biophys. J.*, **53**, 665 (1988).
6. J. Y. Huang, Z. Chen and A. Lewis, *J. Phys. Chem.*, **93**, 3314–3320 (1989).
7. H. E. Katz, C. W. Dirk, K. D. Singer and J. E. Sohn, *Mol. Cryst. Liq. Cryst. Inc. Nonlin. Opt.*, **157**, 525–533 (1988).
8. J. L. Oudar, *J. Chem. Phys.*, **67**, 446–457 (1977).
9. D. J. Williams, *Nonlinear optical properties of organic and polymeric materials* (American Chemical Society, Washington, D.C., 1985).
10. C. W. Spangler, R. McCoy, P. Fleitz, C. F. Zhang and R. R. Birge, in *Molecular Electronics*, (ed. A. Aviram) (Engineering Foundation, New York, in press).
11. K. D. Singer and A. F. Garito, *J. Chem. Phys.*, **75**, 3572–3580 (1981).
12. M. L. H. Green, S. R. Marder, M. E. Thompson, J. A. Bandy, D. Bloor, P. V. Kolinsky and R. J. Jones, *Nature*, **330**, 360–362 (1987).
13. A. B. Myers and R. R. Birge, *J. Chem. Phys.*, **74**, 3514–3521 (1981).
14. N. Hampp, C. Bräuchle and D. Oesterhelt, Proceedings of the Intern. Congress on Optical Science and Engineering, Paris, April 24–28, (1989).
15. R. R. Birge, B. R. Ware, P. A. Dowben and A. F. Lawrence, in *Molecular Electronics*, (ed. A. Aviram) (Engineering Foundation, New York, in press).
16. R. R. Birge, C. F. Zhang and A. F. Lawrence, in *Proceedings of the Santa Clara Conference on Molecular and Biomolecular Electronics*, (ed. F. Hong) (Plenum, New York, in press).
17. G. A. Schick, A. F. Lawrence and R. R. Birge, *Trends Biotech.*, **6**, 159–163 (1988).
18. A. F. Lawrence and R. R. Birge, in *Nonlinear electrodynamics in biological systems*, (eds. H. R. Adey & A. F. Lawrence) pp. 207–218 (Plenum, New York, 1984).
19. R. R. Birge, A. F. Lawrence and L. A. Finsen. *Current research and future potential of the application of molecular electronics to computer architecture*, pp. 3–8 (International Technology Institute, Pittsburgh, Pa., 1986).
20. N. N. Vsevelodov and V. A. Poltoratskii, *Sov. Phys. Tech. Phys.*, **30**, 1235 (1985).
21. D. Oesterhelt and W. Stoeckenius, *Nature (London)*, *New Biol.*, **233**, 149–152 (1971).
22. D. Oesterhelt and W. Stoeckenius, *Methods Enzymol.*, **31**, 667–678 (1974).
23. D. Oesterhelt and L. Schuhmann, *FEBS (Fed. Eur. Biochem. Soc.) Lett.*, **44**, 262–265 (1974).
24. W. Stoeckenius and R. Bogomolni, *Annu. Rev. Biochem.*, **52**, 587–616 (1982).
25. W. Stoeckenius, R. H. Lozier and R. Bogomolni, *Biochem. Biophys. Acta*, **505**, 215–278 (1979).
26. R. H. Lozier, R. A. Bogomolni and W. Stoeckenius, *Biophys. J.*, **15**, 955–962 (1975).
27. R. R. Birge, *Biochim. Biophys. Acta*, (in press).
28. R. R. Birge and C. F. Zhang, *J. Chem. Phys.*, (in press).
29. R. R. Birge, J. A. Bennett, B. M. Pierce and T. M. Thomas, *J. Am. Chem. Soc.*, **100**, 1533–1539, (1978).
30. R. R. Birge, J. A. Bennett, L. M. Hubbard, A. L. Fang, B. M. Pierce, D. S. Kliger and G. E. Leroi, *J. Am. Chem. Soc.*, **104**, 2519–2525 (1982).
31. R. R. Birge, L. P. Murray, R. Zidovetzki and H. M. Knapp, *J. Am. Chem. Soc.*, **109**, 2090–2101 (1987).
32. L. P. Murray and R. R. Birge, *Canadian J. Chem.*, **63**, 1967–1971 (1985).
33. R. R. Birge, L. P. Murray, B. M. Pierce, H. Akita, V. Balogh-Nair, L. A. Finsen and K. Nakanishi, *Proc. Nat. Acad. Sci. USA*, **82**, 4117–4121 (1985).
34. R. R. Birge, *Accts. Chem. Research*, **19**, 138–146 (1986).
35. R. R. Birge, *Methods in Enzymology*, **88**, 522–533 (1982).
36. H. J. Polland, M. A. Franz, W. Zinth, W. Kaiser, E. Kolling and D. Oesterhelt, *Biophys. J.*, **49**, 651–662 (1986).
37. H. J. Polland, M. A. Franz, W. Zinth, W. Kaiser, E. Kolling and D. Oesterhelt, *Biochim. Biophys. Acta*, **767**, 635–639 (1984).
38. R. A. Mathies, J. Lugtenburg and C. V. Shank, in *Biomolecular spectroscopy*, (eds. R. R. Birge & H. H. Mantsch) pp. 138–145 (The International Society for Optical Engineering, Bellingham, Washington, 1989).
39. R. A. Mathies, C. H. Brito Cruz, W. T. Pollard and C. V. Shank, *Science*, **240**, 777 (1988).
40. M. C. Nuss, W. Zinth, W. Kaiser, E. Kolling and D. Oesterhelt, *Chem. Phys. Lett.*, **117**, 1–7 (1985).
41. R. R. Birge, T. M. Cooper, A. F. Lawrence, M. B. Masthay, C. Vasilakis, C. F. Zhang and R. Zidovetzki, *J. Am. Chem. Soc.*, **111**, 4063–4074 (1989).
42. R. R. Birge, in *Ultrasensitive laser spectroscopy*, (ed. D. S. Kliger) pp. 109–174 (Academic Press, Inc., New York, 1983).

43. O. S. Mortensen and E. N. Svendsen, *J. Chem. Phys.*, **74**, 3185–3189 (1981).
44. W. M. McClain and R. A. Harris, in *Excited States*, (ed. E. C. Lim) pp. 1–56 (Academic Press, New York, 1977).
45. D. E. Metzler and C. M. Harris, *Vision Res.*, **18**, 1417–1420 (1978).
46. R. R. Birge and B. M. Pierce, *J. Chem. Phys.*, **70**, 165–178 (1979).
47. B. Dick and G. Hohlneicher, *J. Chem. Phys.*, **76**, 5755–5760 (1982).
48. R. R. Birge, in *Spectroscopy of biological molecules*, (eds. C. Sandorfy & T. Theophanides) pp. 457–471 (D. Reidel, Boston, 1984).
49. R. R. Birge, B. M. Pierce and L. P. Murray, in *Spectroscopy of biological molecules*, (eds. C. Sandorfy & T. Theophanides) pp. 473–485 (D. Reidel, Boston, 1984).
50. L. P. Murray, L. A. Findsen, B. M. Pierce and R. R. Birge, in *Fluorescence in the biomedical sciences*, (eds. D. L. Taylor, A. Waggoner, R. Lannie, R. Murphy & R. R. Birge) pp. 105–127 (Alan R. Liss, New York, 1986).
51. M. B. Masthay, L. A. Findsen, B. M. Pierce, D. F. Bocian, J. S. Lindsey and R. R. Birge, *J. Chem. Phys.*, **84**, 3901–3915 (1986).
52. J. F. Ward, *Rev. Mod. Phys.*, **37**, 1–18 (1965), (see also *Mol. Phys.*, **20**, 513 (1971)).
53. V. J. Docherty and D. Pugh, *J. Chem. Soc. Faraday Trans.*, **2** **81**, 1179–1192 (1985).
54. A. B. Myers, R. A. Harris and R. A. Mathies, *J. Chem. Phys.*, **79**, 603–613 (1983).
55. I. J. Lee, J. K. Gillie and C. K. Johnson, *Chem. Phys. Lett.*, **156**, 227–232 (1989).
56. A. Yariv, *Quantum Electronics, 2nd Edition*, pp. 1–570 (John Wiley & Sons, 1975).